STUDY OF AN IMPROVED BEAM SCREEN DESIGN FOR THE LHC INJECTION KICKER MAGNET FOR HL-LHC*

V. Vlachodimitropoulos[†], M.J. Barnes, L.Ducimetière, L. Vega Cid, W. Weterings,
CERN, Geneva, Switzerland

Abstract

During Run 1 of the LHC, one of the injection kicker magnets (MKIs) occasionally exhibited an excessively high ferrite temperature, caused by coupling of the high intensity beam to the real impedance of the magnet. Beam-screen upgrades have been very effective in reducing beam coupling impedance during Run 2. However, temperature measurements during LHC operation have shown that one end of the MKIs ferrite yoke is consistently hotter than the other: this effect is due to highly non-uniform beam induced power deposition along the kicker. Electromagnetic and thermal simulations show that part of the ferrite yoke will be above its Curie temperature when the LHC is operated with HL-LHC beam parameters, which could increase the turn-around time between fills of the LHC. An impedance mitigation study is presented in this paper with emphasis on the effect of the beam screen layout upon both total beam induced power deposition and its longitudinal distribution. Results of complex thermal simulations, to benchmark the effectiveness of the proposed schemes, are reported. To validate the proposed modification a test bench measurement was performed and preliminary results are discussed.

INTRODUCTION

The MKIs are fast pulsed transmission line kicker magnets of the LHC beam injection system [1]. To shield the ferrite yoke from the beam, by providing a path for the beam image current, a set of 24 conductive wires is placed in the inner part of a ceramic tube along the length of the magnet aperture [2]. Stringent rise-time specifications require that the wires are capacitively coupled to a grounded metallic cylinder at the upstream end of the tube while the downstream end can be directly grounded. Their non-trivial arrangement is dictated by minimization of dielectric breakdowns and flash-overs during High Voltage (HV) pulsing. In addition, an asymmetric vacuum gap was introduced between the capacitively coupled end of the conductive wires and the grounded outer metallic cylinder to improve HV behaviour [3]. To damp low frequency modes, which can be excited along the length of the ceramic tube, two sets of 9 ferrite rings (Ferroxcube [4] 4B3 and 4M2 types are used alternately - see Fig. 1) are placed at each of its ends. The characteristics of the capacitively coupled end of the beam screen design are discussed in greater depth in [2]. A reduced model of the MKI was built with CST Particle Studio [5] and details of its upstream end are shown in Fig. 1.
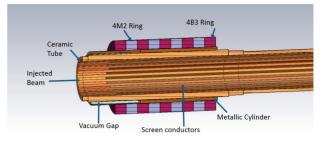
Figure 1: Capacitively coupled end of MKI beam screen.

Table 1: Nominal Beam Parameters

	ppb	t_b (cm)	N_b
Run 2	1.15×10^{11}	7.55	2808
HL-LHC	2.2×10^{11}	7.55	2748

Recent studies have shown that this design has led to a significant reduction of the beam induced heating in the yoke while introducing a non-uniform power deposition along the length of the MKI [6–8]. Observations during Run 2 have verified the expected behaviour and predictions suggest that no heating issue should arise during the run [9]. However, electromagnetic (e/m) and thermal simulations suggest that the ferrite yoke will exceed its Curie temperature (T_C=125 °C) when operated with HL-LHC beam parameters (see Table 1: protons per bunch (ppb), bunch spacing (t_b) and number of bunches (N_b)), leading to long cool down times before a new beam can be safely injected [8]. Thus, upgrades in the design of the MKI beam screen are necessary for unperturbed HL-LHC operation.

BEAM SCREEN ANALYSIS

Heating of the ferrite yoke occurs due to beam power loss, P_L, caused by coupling of the beam spectrum to the real part of the longitudinal beam impedance of the kicker, $\Re\{Z_L\}$, according to the formula

$$P_L = 2I_b^2 \sum_{n=1}^{\infty} |\hat{\lambda}(nf_0)|^2 \Re\{Z_L(nf_0)\}, \qquad (1)$$

where I_b is the average beam current, defined as the total beam charge passing through the device per unit of time, and $\hat{\lambda}(f)$ is the Fourier transform of the normalised longitudinal beam charge distribution evaluated at multiples of the beam revolution frequency, f_0.

Due to the beam screen design, shown in Fig. 1, an open-ended resonating $\lambda/2$ cavity is formed in the region where the screen conductors overlap with the outer metallic cylin-
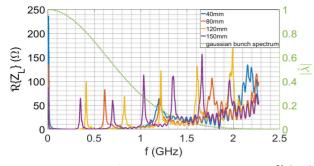
Figure 2: Real part of the longitudinal impedance, $\Re\{Z_L\}$, of MKI for different overlap lengths of the resonating cavity.

Figure 3: Estimated power loss in the MKI as a function of the overlap length for nominal Run 2 beam parameters. Results are normalised to post-LS1 losses P_{ref}.

der: its length, $L_{overlap}$, is defined as the distance between the downstream end of the cylinder and the capacitively coupled end of longest screen conductor. The effective dielectric constant $\epsilon_{r,eff}$ is determined by the alumina tube ($\epsilon_r \approx 10$) and the asymmetric vacuum gap. As a result of the overlap, $\Re\{Z_L\}$ exhibits resonant behaviour [2,6] and the beam looses energy, primarily, at the resonant frequencies of the cavity (Eq. (2))

$$f_n^{res} = n \frac{c}{\sqrt{\epsilon_{r,eff}} 2 L_{overlap}}, \qquad n = 1, 2, ... \qquad (2)$$

Shorter Metallic Cylinder

In the present paper, an attempt is made to reduce P_L by effectively modifying $\Re\{Z_L\}$ and in particular by altering its coupling to the beam spectrum. This can be achieved by shifting the impedance peaks to higher frequencies where the beam power spectrum is reduced. By shortening the length of the outer metallic cylinder, $L_{overlap}$ is decreased and in turn, according to Eq. (2), the resonant frequencies of the cavity, and consequently of the impedance peaks, are upshifted. A similar approach was attempted in [10] where the length of the overlapping region was reduced by decreasing the length of the screen conductors.

Different overlap lengths were simulated and the general expected behaviour of the $\Re\{Z_L\}$ can be seen in Fig. 2 where predictions for four lengths are shown. In the same figure, the envelope of the normalised beam spectrum is shown for a Gaussian bunch profile and Run 2 beam parameters.

A parametric analysis for overlap lengths between 15 mm and 150 mm was performed and the estimated losses were calculated using Eq. (1) and nominal Run 2 beam parameters. The results are plotted in Fig. 3 where a solid line is fitted to the data: the results are normalised to the estimated power loss for the post-LS1 design, P_{ref}. In general, the anticipated tendency for decreasing power loss with shorter overlap lengths is evident. However, the non-monotonic dependence is attributed to the relative position of the impedance peaks to the beam harmonics: peaks at certain frequencies might fall close to a harmonic, thus potentially giving rise to higher losses. The steep increase in P_L for overlaps below 30 mm indicates a reduction of the effectiveness of the beam screen.

Exposing Ferrite Rings

In addition to power loss reduction, shortening the length of the outer metallic cylinder, while maintaining the position of the rings, leads to greater exposure of the ferrite rings to the radiated e/m power. In this way, they act effectively as e/m absorbers that dissipate part of the power radiated from the cavity before it reaches the yoke.

Therefore it is clear that a shorter metallic cylinder has a two-fold impact on the beam induced heating of the MKI yoke: reducing the total beam power loss while at the same time redistributing it, away from the yoke, to the rings that can be cooled more easily [11].

PROPOSED MODIFICATION

Using minimum P_L as a criterion for the optimal overlap length, an overlap of 40 mm was chosen for further analysis and comparison with the current design. With such a change, a reduction in the estimated total power loss of more than 30% is expected. In addition, a redistribution of the power loss along the magnet is foreseen. A comparison of the power deposition in the first 15 most affected ferrites (9 rings + 6 yokes) for the two cases under study is shown in Fig. 4. To highlight relative changes in the deposited power, normalised distributions are displayed.

The effectiveness of the exposure of the rings to the radiated power is clear: the relative power in the first six yokes has been significantly reduced (from 21% to 5% of total power loss) and is now primarily concentrated in the upstream end rings (88% instead of 40%). In the existing post-LS1 design, 9% of the total power loss is deposited in the first yoke and about 13% in the most affected (9th) ring. On the contrary, for the proposed modification the percentage of the power deposited in the first yoke has dropped to nearly 1% while the fourth ring absorbs almost 40% of the total power. Overall, the proposed modification is expected to reduce the power deposited in the first yoke by almost 90%.

THERMAL PREDICTIONS FOR HL-LHC

To validate the effectiveness of the proposed change on expected temperatures, thermal simulations were carried out using the estimated power deposition distributions [11]. To
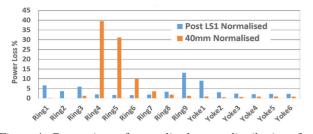
Figure 4: Comparison of normalised power distributions for post-LS1 and proposed, 40 mm overlap, MKI beam screen.

Table 2: Estimated Temperatures

Post-LS1/Proposed Design	Run 2	HL-LHC
Yoke 1st	107/85	240/160
Hottest Ring	145/185	320/390

that end, absolute power data is needed and the normalised power distributions were first scaled with the corresponding total power loss as calculated from Eq. (1). According to previous results [12], Eq. (1) underestimates P_L when $\Re\{Z_L\}$ is obtained from a CST simulation, compared to the same calculation done with $\Re\{Z_L\}$ estimated from a test-bench measurement. To compensate for this discrepancy, and following a worst case scenario approach, a second scaling with an additional factor of 4 was applied to the predicted power deposition data. Scaling by a factor of 4 also results in thermal predictions which are in good agreement with measurements from the LHC [11]. Expected maximum temperatures (in °C) for the first, consistently hottest, ferrite yoke and the hottest ring for the two designs are shown in Table 2, where Run 2 and HL-LHC beam parameters are considered.

The proposed modification would be expected to improve the thermal behaviour of the MKI for Run 2: the hottest yoke temperature is reduced while the anticipated increase in the temperature of the hottest ring is below its T_C (200 °C and 250 °C for 4M2 and 4B3, respectively). However, for HL-LHC, without any cooling, the maximum temperatures of both the ferrite yoke and the hottest ring, the 5th in the proposed configuration, are predicted to significantly exceed their respective T_C. As a result, assuming that above T_C the rings loose their damping properties, some of the rings will stop acting as e/m absorbers, leading to more power being dissipated in the yoke, causing it to reach even higher temperatures. Measurements are planned to assess the influence of temperature upon the frequency dependence of the real and imaginary parts of ferrite permeability.

Nevertheless, a cooling system around the ferrite rings is expected to maintain the temperature of both the rings and yokes below their T_C [11]. Further simulations and measurements are required to validate the predictions.

PRELIMINARY MEASUREMENTS

To verify the expected change in impedance, a test-bench measurement was carried out with a shorter metallic cylin-
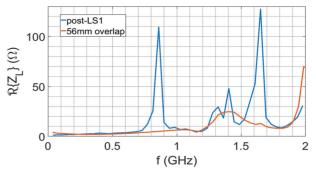

Figure 5: Comparison of the MKI impedance for the two designs using the resonant measurement method.

der. Due to mechanical constraints, an 81-millimetre long cylinder was chosen that led to an overlap of 56 mm. A layer of Kapton around the ceramic tube provided support for the last 5 upstream ferrite rings. The results of the two measurements, using the resonant method [13], are presented in Fig. 5.

Although the resonant method suffers from limited frequency resolution, constrained by the length of the device under test, the improvement in the MKI impedance is evident. With the proposed modification the resonant peaks below 1 GHz seem to disappear leading to a nearly flat real impedance spectrum. However, the first resonant peak was expected to appear around 1.2 GHz; its absence can probably be attributed to the resolution of the method. The remaining but seemingly smoother peak at 1.4 GHz could possibly be an artefact of the measurement. Power loss estimates using Eq. (1) predict a 60% reduction compared to the post-LS1 design. Measurements to verify power redistribution along the magnet are ongoing.

SUMMARY AND FUTURE WORK

Previous e/m and thermal simulations suggested that during HL-LHC operation of the LHC the MKI yokes would exceed their T_C, thus leading to unacceptably long turn-around times between long LHC fills. In the present paper, a simple and easily implemented modification to the MKI design is proposed that can reduce and redistribute power deposition along the kicker, concentrating it in parts that can be cooled relatively easily. According to thermal simulations, the proposed upgrade alone will not be sufficient for HL-LHC operation. Nonetheless, a suitable cooling system is expected to be beneficial in reducing temperatures to acceptable levels. Preliminary results of test bench measurements of the MKI beam coupling impedance, indicate significant reduction in power loss. Measurements to verify the power redistribution are currently ongoing.

ACKOWLEDGEMENTS

REFERENCES

[1] L. Ducimetière, N. Garrel, M.J. Barnes, and G. Wait,"The LHC injection kicker magnet", in *Proc. PAC'03*, Portland, Oregon, USA, May 2003, pp. 1162-1164.

[2] H. Day, "Beam Coupling Impedance Reduction Techniques of CERN Kickers and Collimators", Ph.D. thesis, School of Physics and Astronomy, The University of Manchester, Manchester, United Kingdom, 2013.

[3] M.J. Barnes *et al.*, "Reduction of surface flashover of the beam screen of the LHC injection kickers", in *Proc. IPAC'13*, Shanghai, China, May 2013, pp. 735-737.

[4] http://www.ferroxcube.com

[5] http://www.cst.com

[6] H. Day *et al.*, "Evaluation of the beam coupling impedance of the new beam screen designs for the LHC injection kicker magnets", in *Proc. IPAC'13*, Shanghai, China, May 2013, pp. 1649-1651.

[7] M.J. Barnes *et al.*, "Operational experience of the upgraded LHC injection kicker magnets", in *Proc. IPAC'16*, Busan, Korea, May 2016, pp. 3623-3626.

[8] H. Day, M.J. Barnes, L. Ducimetière, L. Vega Cid, and W. Weterings, "Current and future beam thermal behaviour of the LHC injection kicker magnets", in *Proc. IPAC'16*, Busan, South Korea, May 2016, pp. 3615-3618.

[9] M.J. Barnes *et al.*, "Operational experience of the upgraded LHC injection kicker magnets during Run 2 and future plans", presented at the IPAC'17, Copenhagen, Denmark, May 2017, this conference.

[10] H. Day, M.J. Barnes, L. Coralejo-Feliciano, "Impedance studies of the LHC injection kicker magnets for HL-LHC", in *Proc. IPAC'15*, Richmond, Virginia, USA, May 2015, pp. 370-373.

[11] L. Vega Cid, M.J. Barnes, V. Vlachodimitropoulos, W. Weterings, A. Abánades,"Themal analysis of the LHC injection kicker magnets", presented at the IPAC'17, Copenhagen, Denmark, May 2017, this conference.

[12] H.Day, M.J. Barnes, F. Caspers, E. Metral, B. Salvant, "Impedance reduction techniques in LHC injection kicker magnets", MKI Strategy Meeting, CERN, Geneva, Switzerland, Dec. 2014.

[13] T. Kroyer, F. Caspers, E.Gaxiola, "Longitudinal and transverse wire measurements for the evaluation of impedance reduction measures on the MKE extraction kickers", CERN, Geneva, Switzerland, AB-Note-2007-028.